Available online at www.sciencedirect.com

SciVerse ScienceDirect

Ceramics International 38 (2012) 2429–2436

CERAMICS INTERNATIONAL

www.elsevier.com/locate/ceramint

Evaluation of mechanical reliability of zirconia-toughened alumina composites for dental implants

Dongxu Tang, Hyung-Bong Lim, Ki-Ju Lee, Chi-Hoon Lee, Won-Seung Cho *

School of Materials Science & Eng., Inha University, Incheon 402-751, Republic of Korea

Received 14 October 2011; received in revised form 3 November 2011; accepted 3 November 2011
Available online 9 November 2011

Abstract

Zirconia-toughened alumina composites containing 0–30 vol% of 3Y-TZP were fabricated by sintering at 1600 °C for 2 h in air. The effect of the 3Y-TZP content on the mechanical properties and microstructure of the alumina ceramics was investigated. The fracture toughness and biaxial flexural strength increased as the 3Y-TZP content increased. The Young's modulus decreased with 3Y-TZP content according to the rule of mixture, while the hardness showed the contrary tendency. The Weibull modulus of the Al_2O_3 with 20 vol% 3Y-TZP composite is higher than that of alumina. The residual hoop compressive stress developed in ZTA ceramic composites probably accounts for the enhancement of strength and fracture toughness, as well as for the higher tendency of crack deflection. No monoclinic phase and strength degradation were found after low temperature degradation (LTD) testing. The excellent LTD resistance can be explained by the increased constraining force on zirconia embedded in alumina matrix.

Keywords: D. Al_2O_3; Microstructure; Mechanical property; 3Y-TZP; Residual stress

1. Introduction

Advanced ceramics such as alumina (Al_2O_3) and zirconia (ZrO_2) have been used as dental materials since the 1970s [1]. Compared to metal or polymer dental materials, the esthetic, biocompatibility, chemical inertness and high wear resistance characteristics of ceramics have led to their being widely used as dental implant materials. However, the inherently brittle nature of ceramics has limited their application as implants. With the ongoing developments in the field of dentistry, dental implants with high fracture toughness and fracture strength are required [2].

Alumina has shown excellent wear resistance and biocompatibility, but has low toughness and flexural strength [3]. In order to enhance the mechanical properties of alumina ceramics, numerous studies have been carried out to produce zirconia-toughened alumina (ZTA) ceramics, in which zirconia particles are embedded as a second phase. A considerable amount of research has shown that the addition of zirconia into the alumina matrix can improve the mechanical properties of the composite [4–7].

Several mechanisms were introduced to explain the improved mechanical properties of ZTA ceramics. Transformation toughening is a well-known mechanism, which is induced by zirconia particles undergoing tetragonal (t) → monoclinic (m) phase transformation [9]. This phase transformation, which is accompanied by a volume expansion (~4%) and by shear strain, will cause compressive stress that may develop on a ground surface or in the vicinity of a crack tip. A crack must overcome this clamping constraint on the crack tip in order to propagate, which explains the enhanced fracture resistance of the composites. Microcrack toughening is another well-known mechanism. The microcracks related to the phase transformation can absorb fracture energy by extending the stress field of a propagating crack or deflecting the propagating crack, and can thus increase the fracture energy. Furthermore, the internal residual stresses resulting from the thermal expansion mismatch between the alumina matrix and the zirconia particles can affect the mechanical properties of composites [8,9].

Although ZTA ceramic is a very attractive candidate for dental implants, the phase transformation accompanied by

* Corresponding author. Tel.: +82 32 860 7528; fax: +82 32 862 5546.
E-mail address: wscho@inha.ac.kr (W.-S. Cho).

0272-8842/$36.00
doi:10.1016/j.ceramint.2011.11.009

microcracking can result in some degradation of materials properties such as strength; this kind of degradation is known as low temperature degradation (LTD). This LTD is time dependent and can be accelerated by water or water vapor. The transformation proceeds from the surface to the bulk of the zirconia. This LTD phenomenon is non-negligible and limiting for the application of ceramic implants. A great deal of work has been dedicated to understanding the mechanisms of LTD associated with zirconia, but diverse opinions have been expressed [10]. More attention should be paid to the optimum ZrO_2 content in ZTA composites, in which case the LTD could be restrained effectively; it is also necessary to investigate the effect of ZrO_2 content on the mechanical properties, Weibull modulus, and residual stress of composites.

In this work, ZTA composites with a content of 3Y-TZP ranging from 0 to 30 vol% were prepared. Mechanical properties such as fracture toughness and biaxial flexural strength, Weibull modulus, and residual stress were evaluated. Analysis of biaxial flexural strength after the LTD test was carried out in order to evaluate the hydrothermal stability of the ZTA composites.

2. Experimental procedure

2.1. Preparation of composites

High purity Al_2O_3 (SM8, α-Al_2O_3, >99.99%, 0.6 μm, Baikowski Co., France) and 3Y-TZP (TZ-3YSB-E, 90 nm, Tosho, Japan) were used as starting powders. Four compositions were prepared by adding ZrO_2 into Al_2O_3 matrix at levels of 0 vol% (ZTA 0), 10 vol% (ZTA 10), 20 vol% (ZTA 20) and 30 vol% (ZTA 30). The mixed powders were ball-milled for 24 h in ethanol medium using a plastic jar with Al_2O_3 balls. The slurries were simultaneously dried by rotary evaporator. After being dried and sieved, the powders were uniaxially pressed into rectangular and disk shaped green bodies at 100 MPa; then, powders were cold isostatic pressed (CIP) at 150 MPa. The obtained green compacts were sintered at 1600 °C for 2 h in air. After grinding (400 grit diamond wheel) and polishing (1 μm diamond paste), rectangular specimens with dimensions of 3 × 4 × 40 (mm) and disk specimen samples with diameter of 16 mm and thickness of 1.6 mm were obtained.

2.2. Microstructure characterization and physical and mechanical properties

Crystalline phase analysis was conducted by X-ray diffraction using Cu Kα radiation in the 2θ range of 27–33° and 20–80° with a scanning rate of 2°/min. The microstructures of all composites were observed by SEM after they were thermally etched at 1500 °C for 10 min. The average grain size of the alumina and zirconia grains was determined from the SEM images of randomly selected areas using the linear intercept method [12]. Densities of sintered specimens were measured using Archimedes principle. Young's modulus was measured using the dynamic resonance method.

In this study, the fracture toughness was measured by the single-edge V-notched beam (SEVNB) method. For the SEVNB method, ground and polished rectangular specimens (3 mm × 4 mm × 40 mm) were notched on the surface (3 mm × 40 mm) using a diamond charged cutting wheel, perpendicular to the length of the rectangular bars. The depth of the notches was approximately 0.7 mm, ≤20% of the height of the specimen according to the DIN standard [13]. The notches were sharpened with a razor blade machine using a diamond paste filled into the notch. The sharpened notch root radius of the prepared specimen in the micrograph is approximately 17.5 μm, as can be seen in Fig. 1. Then, the fracture strength of the specimens was measured by the four-point flexure test. The hardness was determined from the Vickers indentations. Specimens were polished to mirror-like planes and then indentations were introduced on the surface of specimens of each composition by Vickers hardness testing machine (Akashi, Model, AVK-C0), under 98 N load at a dwell time of 15 s. Biaxial flexural strength was evaluated by piston-on-three-ball test [19]. The disk type specimens were ruptured using a universal testing machine under a cross head speed of 0.5 mm/min. The Weibull distribution of the biaxial flexural strength for ZTA0 and ZTA20 (30 specimens for each composition) was investigated to evaluate the reliability of the ZTA composites. The residual stresses developed in the alumina matrix were also estimated.

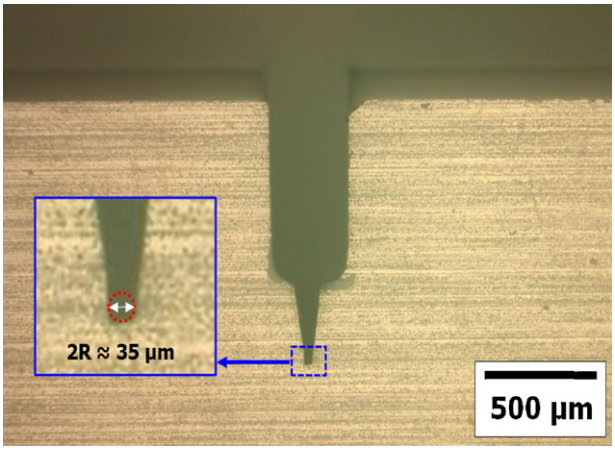

Fig. 1. Example of sharpened V-notch in ZTA specimen.

2.3. Low temperature degradation behavior of ZTA composites

Prior to the low temperature degradation (LTD) test, the disk specimens were polished to a mirror-like plane and were annealed at 1200 °C for 1 h in air to eliminate the stress-induced transformed layer. Subsequently, specimens of each composition were immersed in hot water and kept in autoclave for 36 h. It was estimated that this treatment at 134 °C for 1 h corresponds to ~4 years in vivo [28]. The biaxial flexural strength test and XRD analysis were conducted after the LTD test.

3. Results and discussion

Fig. 2 shows the relative density as a function of the 3Y-TZP content. Based on our preliminary experiment on the sintering

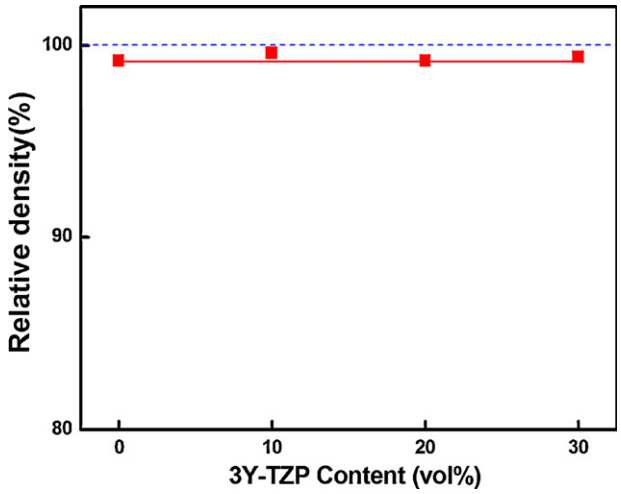

Fig. 2. Effect of the 3Y-TZP content on the relative density of the sintered samples.

conditions, both the monolithic Al_2O_3 and ZTA composites had good sintering ability at 1600 °C. Thus, the specimens were sintered at 1600 °C for 2 h. It is clear that the relative density of all composites was higher than 99.2%, and that all were almost completely densified. The relative densities of each composite showed a substantially similar value, taking into account the experimental error. It can be concluded that the addition of 3Y-TZP had little influence on the densification of Al_2O_3.

Fig. 3 shows the elastic modulus and hardness of composites as a function of 3Y-TZP content. The measured elastic modulus decreased with increase of 3Y-TZP content from 0 to 30 vol%. This increase is reasonable considering that the elastic modulus of Al_2O_3 (400 GPa) is much higher than that of ZrO_2 (192 GPa) [25]. In ceramic matrix composites, the elastic modulus obeyed the linear rule of mixtures [9], which can be explained by Eq. (1):

$$E_{com} = E_A V_A + E_Z V_Z \quad (1)$$

where E_{com} is the elastic modulus of ZTA composites, E_A is the elastic modulus of Al_2O_3, E_Z is the elastic modulus of 3Y-TZP, and V_A and V_Z are the volume fraction of Al_2O_3 and 3Y-TZP, respectively. As can be seen in Fig. 3, the experimental values were consistent with the linear rule of mixtures (dotted line). The elastic modulus decreases with the volume faction of porosity, as shown in the following relationship (2) [26]:

$$E = E_0(1 - 1.9P + 0.9P^2) \quad (2)$$

where E is the elastic modulus of porous ceramic, E_0 is the elastic modulus of the nonporous ceramic, and P is the porosity. The elastic moduli for zero porosity were estimated using Eq. (2). The estimated moduli were higher than experimental values. The values of hardness varied from 1840 kg/mm^2 for monolithic Al_2O_3 to 2060 kg/mm^2 for ZTA30 composite. According to the rule of mixture, the calculated values should decrease with the increase of ZrO_2 content because the hardness of high purity alumina is higher than that of 3Y-TZP [2,12,15]. Contrary to expectation, the hardness was found to linearly increase with the content of 3Y-TZP. This can be explained in terms of the stress-induced phase transition of the metastable tetragonal ZrO_2 phase to the stable monoclinic phase. With indentation loading, volume expansion of ~4% and shear strain of ~6% occurred as a result of the stress-induced phase transition in the vicinity of the Vickers indent. These factors of volume expansion and shear strain generate a compressive surface stress field in the surrounding matrix [18], which can result in close up of median cracks during unloading. The increase of the hardness can be also related to the decrease of the grain size of alumina as shown in Fig. 5. The dependence of hardness on grain size of ceramics has been reported by Rice [17] to correspond to an approximate Hall–Petch relation (i.e. $H_V \sim 1/L^{1/2}$, where L is grain size). They reported that Vickers hardness decrease with increasing grain size (L) for finer grain alumina (<10 μm), and become insensitive to grain size for coarser grain alumina (>10 μm). In this study, the grain size of alumina decreased from 3.0 μm for the monolithic Al_2O_3 to 1.8 μm for the ZTA30.

Fig. 4 presents the effect of the 3Y-TZP content on the fracture toughness and the biaxial strength of the sintered samples. The SEVNB method, used in this study, is much more

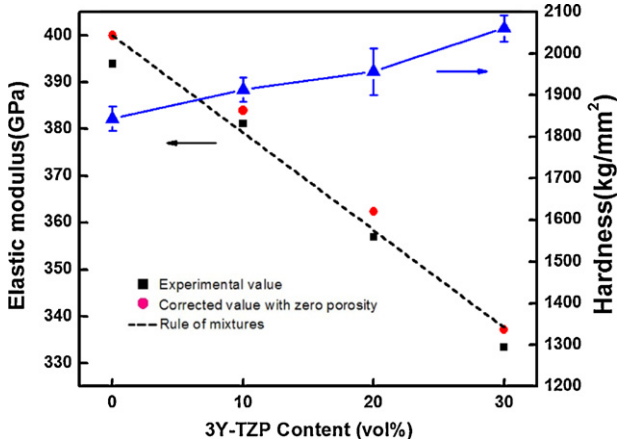

Fig. 3. Effect of the 3Y-TZP content on the elastic modulus and hardness of the sintered samples.

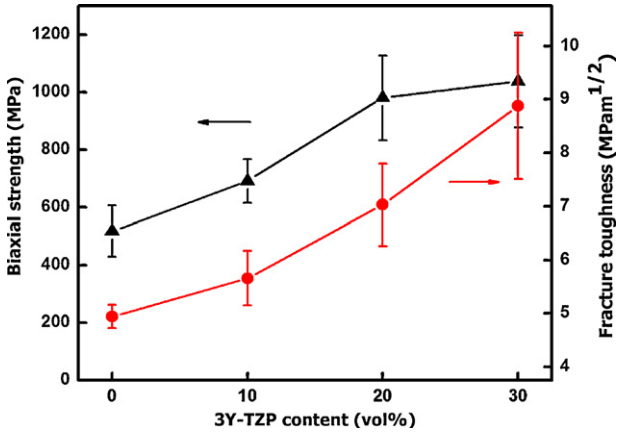

Fig. 4. Effect of the 3Y-TZP content on the biaxial flexural strength and the fracture toughness (SEVNB method) of the sintered samples.

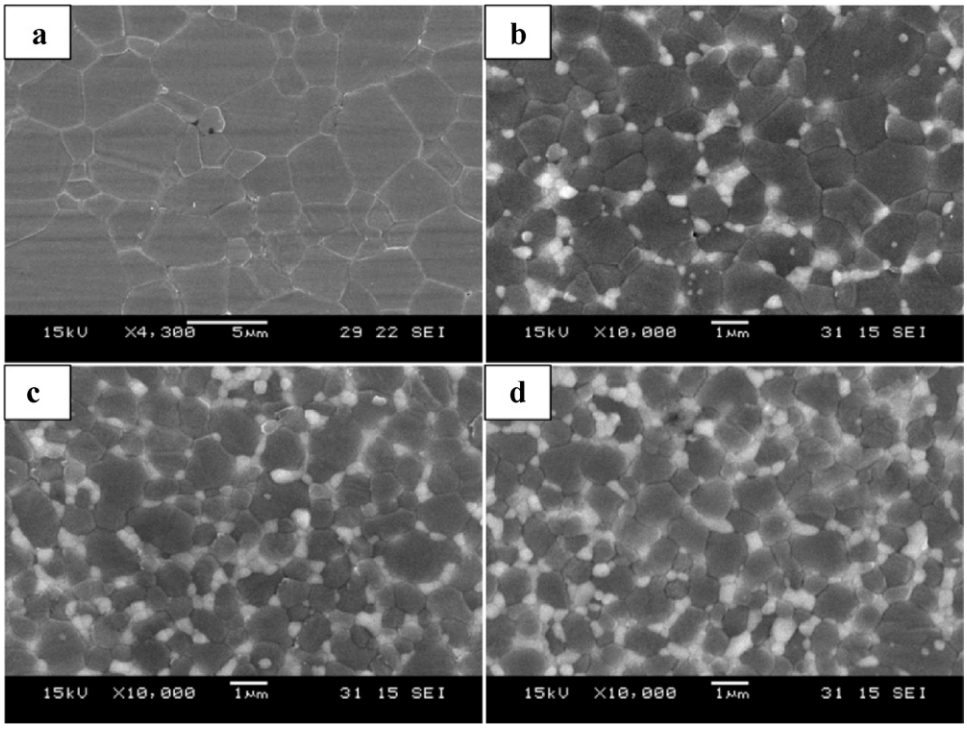

Fig. 5. SEM micrographs of ZTA composites sintered at 1600 °C for 2 h: (a) ZTA0, (b) ZTA10, (c) ZTA20, and (d) ZTA30. The Al_2O_3 and ZrO_2 grains are the darker and brighter phase, respectively.

reliable at measuring fracture toughness than are other methods. Also, this method is less time consuming, and does not require the preliminary study of cyclic compression conditions for fatigue cracks [8]. The fracture toughness increased non-linearly with the 3Y-TZP content, ranging from 0 vol% to 30 vol%, varying from 4.9 to 8.9 MPa $m^{1/2}$. It is obvious that the addition of 3Y-TZP particles into the Al_2O_3 matrix enhances the fracture toughness. This fracture toughness enhancement can be explained by the stress-induced phase transformation of ZrO_2 from tetragonal to monoclinic form; the transformation induced volume expansion generates a compressive stress field that impedes the propagation of cracks and extra load (or work) must be supplied for further crack propagation [3–6].

The biaxial flexural strength also increased with the 3Y-TZP content. According to the fracture mechanics for brittle ceramics, the strength of the ceramic depends on the fracture energy, fracture origin and Young's modulus. The strength was also influenced by microstructural elements such as grain size. A finer grain size results in a higher fracture strength. Thus, the effect of the 3Y-TZP content on the grain size of Al_2O_3 was investigated. Fig. 5 presents micrographs of the ZTA composites with various levels of 3Y-TZP content. Two distinct phases, Al_2O_3 (the darker phase) and ZrO_2 (the brighter phase), could be clearly observed. The grain size of the Al_2O_3 decreased with increasing amounts of 3Y-TZP. It is well known that the second phase impedes the grain growth of the matrix due to the Zener effect [14]. This result is consistent with those in studies carried out by other researchers [15–17]. The grain size of the alumina matrix was investigated using the linear intercept method. The grain size decreased from 3.0 μm for monolithic Al_2O_3 to 1.8 μm for ZTA30. Zirconia particles were homogeneously dispersed in the alumina matrix. It can be observed that two types of zirconia particles, faceted intergranular zirconia particles and spherical intragranular zirconia particles, existed in the alumina matrix. Most of the intergranular zirconia particles were located at the triple junction and the grain boundary of alumina. This was due to their being dragged by the migration of alumina grain boundaries [9]. It is noteworthy that the intragranular zirconia particles with smaller size, less than 0.2 μm, were frequently observed, especially in the ZTA10 composite. The intragranular zirconia particles presented a spherical geometry. This is reasonable considering that zirconia particles with small size could easily be embedded with large alumina grains during grain growth [11].

In addition to toughening mechanisms such as transformation toughening and microcracking, crack deflection was also considered as a possible mechanism. The Vickers indentation was introduced on the polished surface of the ZTA composites to observe the crack deflection. Fig. 6 shows the advancing crack morphologies. The crack advanced in a straight path in monolithic Al_2O_3, while the crack advanced in a zigzag fashion in ZTA composites, showing a higher degree of crack deflection than that in monolithic Al_2O_3. ZTA composites revealed a higher tendency for intergranular crack propagation than did monolithic Al_2O_3. Therefore, the causes of the enhanced strength are thought to be the decreased grain size, the crack deflection and the transformation toughening, etc.

The reliability of ceramics is an important factor for their application in the field of dental implants. Thus, the Weibull modulus was evaluated according to ISO standards [19]. All specimens were annealed at 1200 °C for 1 h to eliminate the residual transformed layer generated during grinding and

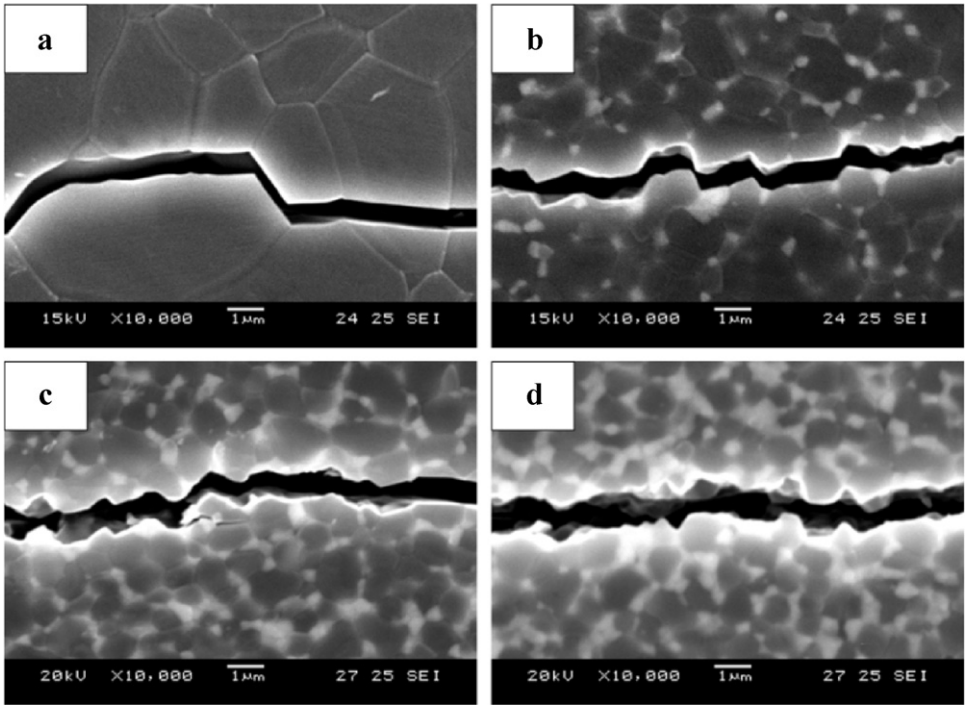

Fig. 6. Crack paths in the ZTA composite: (a) ZTA0, (b) ZTA10, (c) ZTA20, and (d) ZTA30.

polishing; then, 30 specimens for each ceramic specimen were fractured using the biaxial flexural test. Fig. 7 shows the Weibull plots for alumina and for the ZTA20 composite. The Weibull modulus of the ZTA20 sample was higher (7.8) than that of alumina (6.78), indicating a little enhanced reliability in the ZTA20 composite. It was recognized that most of data points for alumina are well fitted by the least-square method. This means that the Weibull modulus did not depend on the stress level. In contrast, the strength distribution for ZTA20 seemed to be bimodal or to exhibit non-Weibull distribution. It has been reported that internal compressive stresses can affect the strength distribution [22].

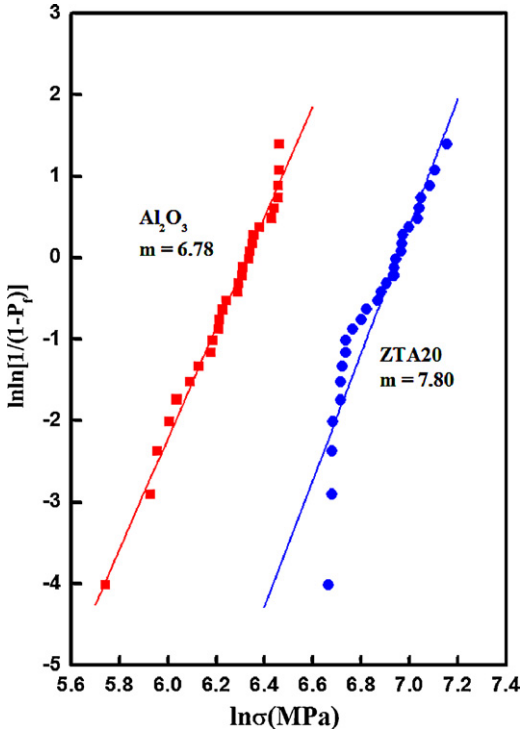

Fig. 7. Weibull plots of the ZTA composites. The solid lines are calculated from a least-squares fit of the data.

The mechanical properties of ceramic composites are influenced by the residual stress, which depends on several factors. These factors are the reinforcement volume fraction, the reinforcement geometry, the mismatch of thermal expansion coefficient ($\Delta\alpha = \alpha_r - \alpha_m$), the temperature interval, and the modulus ratio, E_r/E_m, for which the subscripts r and m denote the reinforcement and the matrix, respectively [20]. Residual stress in ZTA composites can be introduced due to the mismatch of the thermal expansion values for ZrO_2 and Al_2O_3, which values are $10.3 \times 10^{-6}/^{\circ}C$ and $8.1 \times 10^{-6}/^{\circ}C$, respectively. Fig. 8 provides a schematic illustration of the residual stress and the interparticle spacing in ZrO_2 reinforced Al_2O_3 composite. Radial tensile stress and hoop compressive stress developed in the ZTA composites due to the thermal expansion mismatch between 3Y-TZP and Al_2O_3. In such a case, a crack is deflected away from 3Y-TZP particles, resulting in a tortuous crack path, as can be seen in Fig. 6. The radial tensile stress (σ_{rm}) and the hoop compressive stress ($\sigma_{\theta m}$) are described by the following equations, Eqs. (3) and (4) [20]:

$$\sigma_{rm} = \frac{P}{1 - V_p}\left(\frac{a^3}{r^3} - V_p\right), \quad V_p = \left(\frac{a}{b}\right)^3 \tag{3}$$

$$\sigma_{\theta m} = -\frac{P}{1 - V_p}\left(\frac{1}{2}\frac{a^3}{r^3} + V_p\right) \tag{4}$$

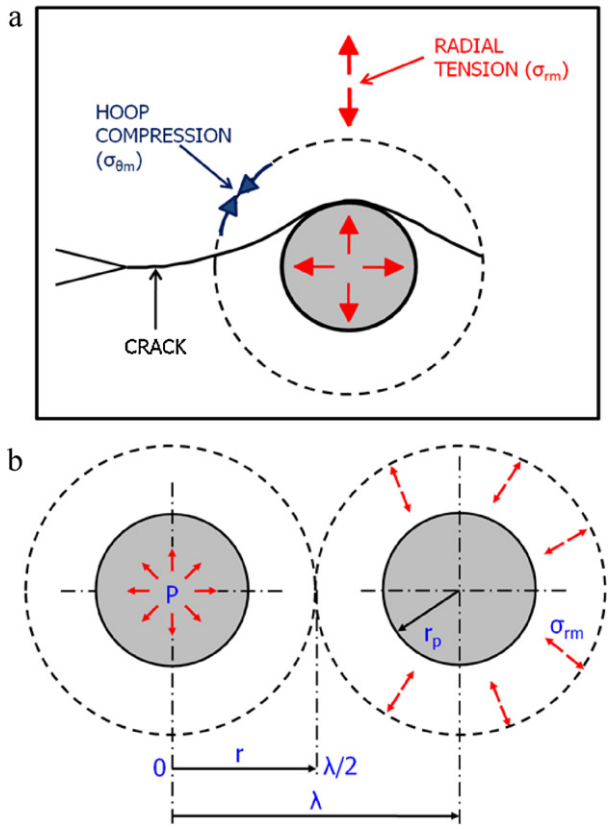

Fig. 8. Schematic illustration for the residual stress and interparticle spacing in ZTA composite: (a) radial tensile stress and hoop compressive stress developed in the ZTA composites due to the thermal expansion mismatch between 3Y-TZP (10.3×10^{-6}/°C) and Al_2O_3 (8.1×10^{-6}/°C), (b) interparticle spacing in ZTA composite.

Table 1
Calculated interparticle spacing in ZTA composite.

Sample	r_p (μm)	λ (μm)	λ/2 (μm)
ZTA10	0.065	$\lambda = \left(\frac{4\pi r_p^3}{3V_p}\right)^{1/3}$	0.078
ZTA20			0.062
ZTA30			0.054

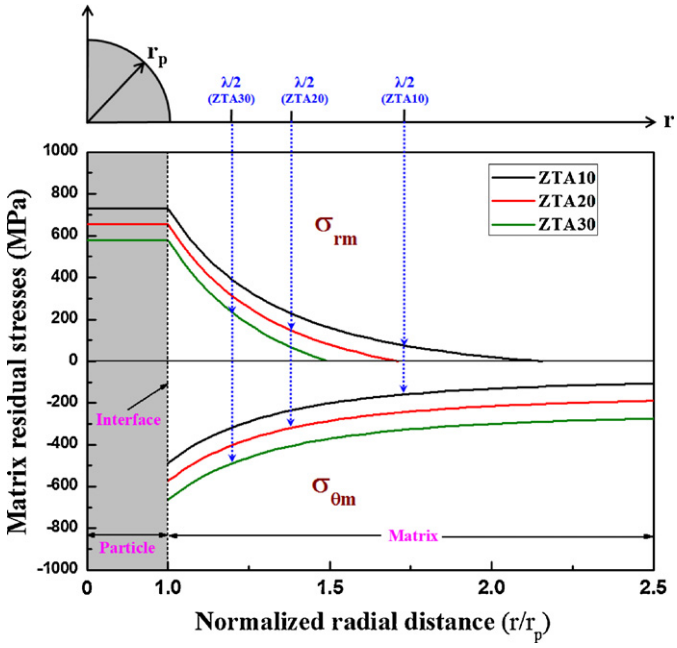

Fig. 9. Calculated radial and hoop stresses in ZTA composites as a function of 3Y-TZP content. The radial distance was normalized by dividing it by the particle radius.

where a is the particle radius, b is the matrix radius, r is the distance, V_p is the volume fraction of the particle in the matrix, and P is the interfacial pressure.

The interfacial pressure P can be evaluated by Eq. (5) [20]:

$$P = \frac{(\alpha_m - \alpha_p)\Delta T}{[(0.5(1+\nu_m) + (1-2\nu_m)V_p)/ (E_m(1-V_p)) + (1-2\nu_p)/(E_p)]}, \quad \Delta T = -1200\,^{\circ}\mathrm{C} \tag{5}$$

If we assume that the dispersed particles form a cubic array, the interparticle spacing λ, which is the distance between the neighboring particles, is given by Eq. (6) [23]:

$$\lambda = \left(\frac{4\pi r_p^3}{3V_p}\right)^{1/3} \tag{6}$$

where r_p and V_p are the radius and volume fraction of the particle, respectively. The calculated interparticle spacing of ZTA ceramic composites are listed at Table 1. The interparticle spacing decreased from 0.156 μm for the ZTA10 sample to 0.108 μm for the ZTA30 sample.

The values of calculated matrix residual stress (radial tension and hoop compressive stresses) in ZTA composites as a function of the 3Y-TZP content are shown in Fig. 9. The radial distance, r, away from the center of the particle, was normalized by dividing it by the particle radius (r_P). At the interface between the particle and the matrix ($r = r_p$) or at a radial distance less than the particle radius ($r < r_p$), the radial tensile stresses (σ_{rm}) maintained constant values and decreased with the 3Y-TZP content. For example, the radial tensile stress decreased from 730 MPa for 10 vol% 3Y-TZP content to 580 MPa for 30 vol% 3Y-TZP content. At the interface between the particle and the matrix, the hoop compressive stress ($\sigma_{\theta m}$) increased with the 3Y-TZP content. For example, the hoop compressive stress increased from 487 MPa for 10 vol% 3Y-TZP content to 663 MPa for 30 vol% 3Y-TZP content. When the distance is larger than the particle radius ($r > r_p$), both the radial tensile stress and the hoop compressive stress decreased with the distance.

It can be concluded that the residual hoop compressive stress developed in ZTA ceramic composites probably accounts for the enhancement of strength and fracture toughness, as well as for the higher tendency of crack deflection.

On the other hand, LTD testing is essential to confirm the composite's suitability for application as a dental material. As an LTD test at 134 °C for 1 h corresponds to ~4 years in vivo, numerous studies about LTD have been conducted at this

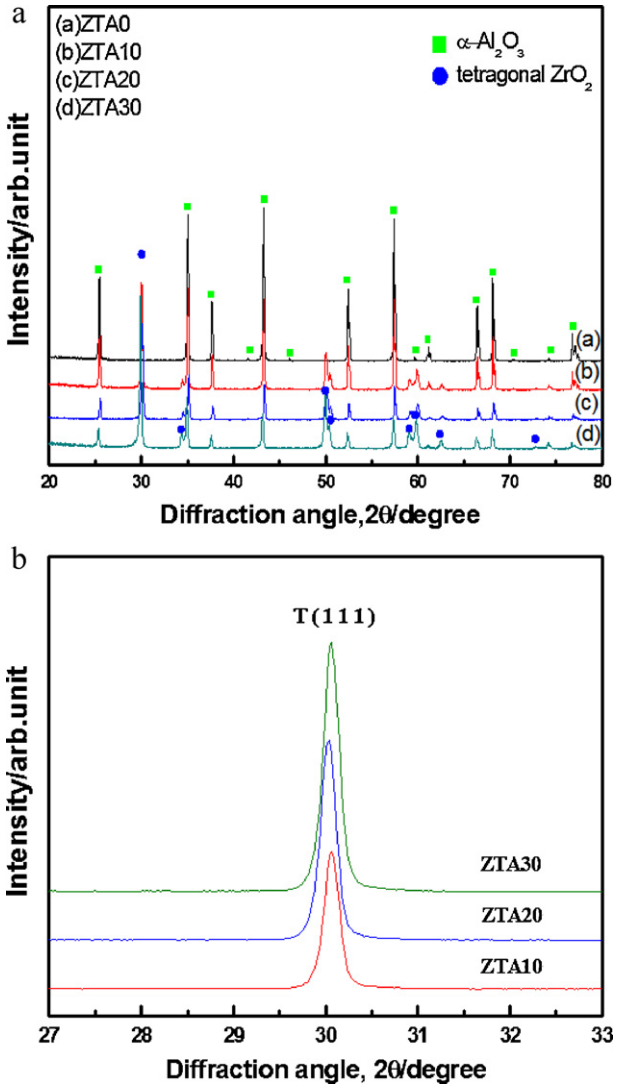

Fig. 10. X-ray diffraction patterns of the ZTA composites before/after LTD test at 134 °C for 36 h in autoclave; (a) as-sintered specimens before LTD test, and (b) Al_2O_3/3Y-TZP specimens after LTD test.

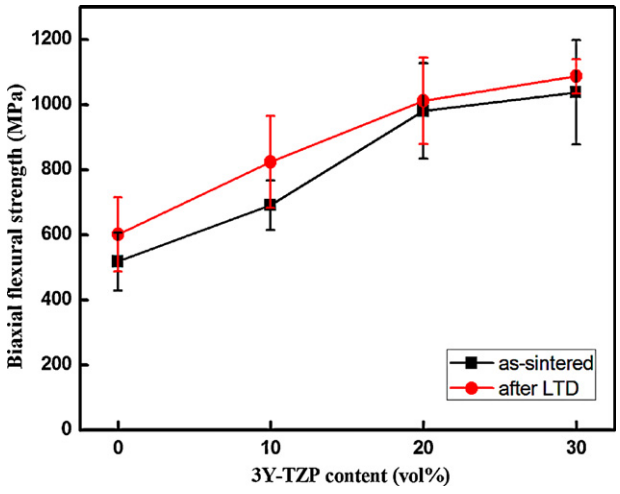

Fig. 11. Biaxial flexural strength values for the as-sintered specimens and the specimens after the LTD test at 134 °C for 36 h in autoclave, as a function of the 3Y-TZP content.

temperature [10]; in this study, the condition for the LTD test of the ZTA composites was set at 134 °C for 36 h in water. The biaxial strengths of the ZTA composites after the LTD test were investigated. Then, XRD analysis was conducted to examine the phase transformation into monoclinic phase. Fig. 10 shows the XRD patterns of the ZTA composites before (a) and after (b) the LTD test. Before the LTD test, the α-Al_2O_3 and the tetragonal ZrO_2 phase were observed as major phase and minor phase, respectively. Fig. 10(b) shows the results of XRD analyses for the ZTA composites after the LTD test. The XRD analyses were conducted under a narrow range of diffraction angles, from 27° to 33°, because the monoclinic zirconia phase can be easily substantiated by diffraction peaks at $2\theta = 28.06°$ and 31.24° [27]. It is clear that no diffraction peaks corresponding to monoclinic ZrO_2 phase were observed. The absence of the monoclinic ZrO_2 phase indicates that the composites had an enhanced hydrothermal stability. This enhanced hydrothermal stability is considered to arise from the constraining force of the harder alumina matrix [21]; the tetragonal ZrO_2 particles need to overcome a critical stress to trigger the transformation. In ZTA composites, the stability of tetragonal zirconia increased due to the Al_2O_3 matrix with higher Young's modulus. The surrounding harder matrix increased the constraining force on the zirconia particles. The constraining force made it more difficult for tetragonal ZrO_2 to transform, thus enhancing the LTD resistance of the ZTA composites.

Fig. 11 shows the biaxial strength of the samples before and after the LTD test. The degradation of strength was not observed after the LTD test. This result is consistent with those in Tsukama's study [24]. He found that the phase transformation from tetragonal to monoclinic due to ageing was not observed on the surface of the sintered material with an Y_2O_3 content of 2.6 mol% and a grain size smaller than 0.5 μm. Furthermore, no significant strength degradation was observed when the Y_2O_3 content was above 2.2 mol% and the grain size was smaller than 0.5 μm. Thus, it can be concluded that both the higher amount of Y_2O_3 (3 mol%) and the smaller grain size (<0.5 μm) improve the hydrothermal stability of zirconia, as in the present study.

4. Conclusions

Al_2O_3/3Y-TZP composites containing 0–30 vol% of 3Y-TZP were fabricated by pressureless sintering; the effect of the 3Y-TZP content on the mechanical properties and microstructure of Al_2O_3 ceramics was evaluated. The following results were obtained.

1. Both the monolithic Al_2O_3 and Al_2O_3/3Y-TZP composites presented a high sintering ability. ZrO_2 particles dispersed homogenously in the Al_2O_3 matrix in all composites, and acted as inhibitor for the grain growth of Al_2O_3.
2. Young's modulus decreased with the increase of the 3Y-TZP content according to the linear rule of mixtures. Hardness

was found to linearly increase with the content of 3Y-TZP due to the compressive surface stress field generated by the stress-induced phase transition. The fracture toughness and the biaxial flexural strength increased with the 3Y-TZP content. Residual hoop compressive stress developed in the ZTA ceramic composites, probably accounting for the enhancement of strength and fracture toughness, as well as for the higher tendency of crack deflection.

3. No monoclinic phase and strength degradation were found after the LTD test. The excellent LTD resistance can be explained by an increased constraining force on zirconia embedded in the alumina matrix.

Acknowledgements

This study was supported by the Basic Science Research Program through the National Research Foundation of Korea (NRF), funded by the Ministry of Education, Science and Technology (2010-0015792).

References

[1] C. Santos, L.H.P. Teixeira, Mechanical properties and cytotoxicity of 3Y-TZP bioceramics reinforced with Al_2O_3 particles, Ceram. Int. 35 (2009) 709–718.
[2] A.N. Rascon, A.A. Elguezabal, On the wide range of mechanical properties of ZTA and ATZ based dental ceramic composite by varying the Al_2O_3 and ZrO_2 content, Int. J. Refract. Met. Hard Mater. 27 (2009) 962–970.
[3] A.H. De Aza, J. Chevalier, R. Torrecillas, Crack growth resistance of alumina zirconia and zirconia toughened alumina ceramics for joint prostheses, Biomaterials 23 (2002) 937–945.
[4] F.F. Lange, Transformation toughening. Part 4. Fabrication, fracture toughness and strength of Al_2O_3–ZrO_2 composites, J. Mater. Sci. 17 (1982) 247–254.
[5] M. Yoshimura, S. Somiya, Strength-toughness relations in sintered and isostatically hot-pressed ZrO_2-toughened Al_2O_3, J. Am. Ceram. Soc. 69 (1986) 169–172.
[6] A.G. Evans, Perspective on the development of high-toughness ceramics, J. Am. Ceram. Soc. 73 (1990) 187–206.
[7] B.L. Karihaloo, Contributions of t–m phase transformation to the toughening of ZTA, J. Am. Ceram. Soc. 74 (1991) 1703–1706.
[8] D. Casellas, I. Rāfols, L. Llanes, M. Anglada, Fracture toughness of zirconia–alumina composites, Int. J. Refract. Met. Hard Mater. 17 (1999) 11–20.
[9] J. Wang, R. Stevens, Zirconia-toughened alumina (ZTA) ceramics, J. Mater. Sci. 24 (1989) 3421–3440.
[10] S. Deville, J. Chevalier, G. Fantozzi, Low-temperature ageing of zirconia-toughened alumina ceramics and its implication in biomedical implants, J. Eur. Ceram. Soc. 23 (2003) 2975–2982.
[11] D.D. Jayaseelan, D.A. Rani, Powder characteristics sintering behavior and microstructure of sol–gel derived ZTA composites, J. Eur. Ceram. Soc. 20 (2000) 267–275.
[12] M.C. Moraes, C.N. Elias, J.D. Filho, L.G. Oliveira, Mechanical properties of alumina–zirconia composites for ceramic abutments, Mater. Res. 7 (2004) 643–649.
[13] DIN 51109, Prufung von keramischen Hochleistungswerkstoffen, Ermittlung der Risszahigkeit KIc, Beuth-Verlag, Berlin, 1991.
[14] D. Fan, L.Q. Chen, S.P. Chen, Numerical simulation of zener pinning with growing second-phase particles, J. Am. Ceram. Soc. 81 (3) (1998) 526–532.
[15] F.F. Lange, M. Hirlinger, Hindrance of grain growth in Al_2O_3 by ZrO_2 inclusions, J. Am. Ceram. Soc. 67 (1983) 164–168.
[16] G.N. Hassold, E.A. Holm, D.J. Srolovitz, Effects of particle size on inhibited grain growth, Scr. Metall. 24 (1990) 101–106.
[17] R.W. Rice, Treatise on Materials Science and Technology, Academic Press, New York, 1977, pp. 199–203.
[18] A.G. Evans, Perspective on the development of high-toughness ceramics, J. Am. Ceram. Soc. 73 (2) (1990) 187–205.
[19] ISO 6872.2008 (E), Third Edition, 2008-09-01.
[20] K.K. Chawla, Ceramic Matrix Composites, Chapman & Hall, 1993, pp. 274–279.
[21] G. Pezzotti, V. Sergo, O. Sbaizero, N. Muraki, Strengthening contribution arising from residual stresses in Al_2O_3/ZrO_2 composites: a piezo-spectroscopy investigation, J. Eur. Ceram. Soc. 19 (1999) 247–253.
[22] R. Danzer, P. Supancic, J. Pascual, T. Lube, Fracture statistics of ceramics – Weibull statistics and deviations from Weibull statistics, Eng. Fract. Mech. 74 (2007) 2919–2932.
[23] U.F. Kocks, On the spacing of dispersed obstacles, Acta Met. 14 (1966) 1629–1630.
[24] K. Tsukama, Thermal stability of Y_2O_3-partially stabilized zirnonia (Y-PSZ) and Y-PSZ/Al_2O_3 composites, J. Mater. Sci. Lett. 4 (1985) 857–861.
[25] J.W. Adams, Young's modulus, flexural strength, and fracture of yttria-stabilized zirconia versus temperature, J. Am. Ceram. Soc. 80 (4) (1997) 903–908.
[26] D. William, Callister, Materials Science Engineering: An Introduction, 7th ed., John Wiley & Sons (Asia) Pte Ltd., 2007.
[27] M.C. Lorente, S.S. Scherrer, P. Ammann, Low temperature degradation of a Y-TZP dental ceramic, Acta Biomater. 7 (2011) 858–865.
[28] C.B. Cales, J.M. Drouin, Low temperature aging of Y-TZP ceramics, J. Am. Ceram. Soc. 82 (1999) 2150–2154.